Concept analysis of a frequency-sweeping delta/ sigma beam-switching radar using machine learning

Mohammad Reza Seidi Goldar [#1], Jamshid Hassanpour[*2], Joachim Oberhammer [#3]

[#] School of Electrical Engineering and Computer Science, KTH Royal Institute of Technology, Sweden

[*] School of Electrical and Computer Engineering, University of Tehran, Iran

{[1]mrsg, [3] joachimo}@kth.se, [2]hassanpourjamshid@ut.ac.ir

***Abstract*— This paper investigates a novel radar concept that is based on a minimalistic, small-aperture antenna array but features intelligent beam-shape switching and artificial-intelligence signal processing. In contrast to conventional phased-arrays, size, cost, and hardware complexity are drastically reduced by the proposed dual-antenna array which can create a broad and a frequency-scanning notched beam shape. The angular-resolution and target discrimination performance of the proposed radar concept have been validated by radar simulations for single and multiple target scenarios. For the signal processing, two convolutional neural networks (CNN) and a multilayer perceptron model are benchmarked against each other. A further CNN is implemented for estimating the number of targets, which can be used to pre-select the type of network determining range and cross-range of multiple targets. This paper shows that a small antenna aperture frontend in combination with beam-shape switching and artificial-intelligence signal processing methods is a suitable hardware-efficient radar concept for accurate multi-target location.**

***Keywords*—RADAR, beam-switching, frequency sweeping, notched beam, deep Learning.**

I. INTRODUCTION

Radar target detection and discrimination require identifying several objects and associate range and angular position coordinate to them, with range/angular resolution and accuracy determined by the radar performance. Target localization has various civilian and defence applications [1]-[3]. Alternative applications of a typical radar frontend are communication channel estimation or imaging applications including detection of concealed weapons [4, 5]. Electronically steered phased-array radars [6, 7] are widely used due to their narrow, scanning main lobe which can be accurately positioned over a wide field of view for resolving individual targets. However, phased-array radars require a large aperture and have a high hardware complexity, due to the need for phase-controlling of individual antenna elements [10, 11].An early frequency-beam-scanning array was proposed already in 1966 [8]. Another application of this concept was shown in 1979 by [9] using an x-band microstrip array. In [12] a parallel-plate waveguide-based leaky-wave antenna, integrated with a planar reflector in a micromachining process, was used to steer the antenna radiation pattern from 220 to 300 GHz. Substrate integrated waveguide (SIW) technology has also been explored for beam-steering [13-15]. Multi-static radar systems using sparsely populated antenna arrays provide a way for high positional accuracy at significantly reduced hardware complexity as compared to a fully-populated phased array but requires extensive time-multiplexing and computational complexity which drastically impacts the radar response time, and cannot handle objects moving fast relative to the array scanning time [16]. Many radar detection problems suffer from high computational complexity, which can originate from the radar concept, noisy data collection, nonlinear parameters, and poor resolution [18]. In [19] an adaptive signal processing approach was implemented for solving the inverse scattering problem for characterizing material properties Artificial Neural Networks (ANN) have shown the ability to overcome such problems. Convolutional Neural Networks (CNN) was used as an approved substitute for solving iterative inverse scattering problems at a lower cost of time and computation costs [20], and an electromagnetic inversion problem was transposed into a solvable problem using a Deep-CNN network [21]. These results show an outstanding performance where conventional methods often fail due to challenges of high dimensional problems, nontrivial selection of starting points, and finding the false local minimum. Besides, neural networks have established themselves in feature extraction and prediction problems, for instance, implemented a CNN to find specific features of a hand gesture without beam steering [21]. Analyzing time-sequential signal frames further assists to classify gestures from otherwise non-deterministic radar signals.

This paper presents a new radar concept, which in contrast to utilizing a large antenna-aperture and large hardware-complexity phased arrays, utilizes only two antenna elements but features beam-shape switching and frequency-sweeping. In combination with an artificial-intelligence algorithm trained on the radar signals from the two beam shapes, it is hypothesized that this radar architecture gives sufficient information for separating multiple targets in range and angle, despite its minimalistic aperture.

II. RADAR FRONT-END CONCEPT

The radar concept presented in this paper is based on a frequency-sweeping dual-antenna front-end, with a physical antenna pitch of 0.75λ at the center frequency to get optimum main patter, and a very small overall antenna aperture of only 1.25 λ (at the center frequency), using open-ended waveguides. The antennas are fed from the same signal source via a power splitter, and one of the antennas has an additional delay line of 13 λ inserted, which results in a frequency-depending phase difference and thus beam-steering of the relatively wide main lobe with an average Half Power Beam Width (HPBW) of

28.75˚. In the following, this beam shape is referred to as sigma or broad beam. In addition to this broad-beam sweeping, a second beam-shape is used by steering the otherwise identical antenna-network in anti-phase, resulting in a notched beam [17] which also scans over the field of view by frequency sweeping, which is in the following referred to as the delta beam shape.

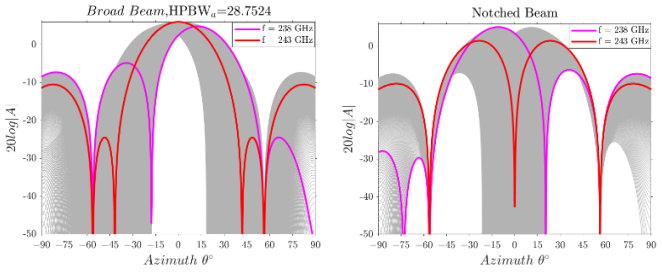

(a) (b)

Fig. 1. Beam-shapes: (a) frequency-swept broad beam (sigma beam) created by two slot antennas at a pitch of 0.75 λ; (b) frequency-swept notched beam (delta beam), with anti-phase antenna steering. Red=radiation pattern at centre frequency (243 GHz), purple=pattern at lower end of the band (238 GHz), gray=radiation patterns when scanning from 238-248 GHz.

The radar is operated with a stepped-frequency waveform with a 25 MHz frequency increment over a bandwidth of 10 GHz from 238-248 GHz (frequency range according to specifications in this research project). The azimuth-plane radiation pattern of the sigma beam is shown in Fig. 1a, and of the delta beam is shown in Fig. 1b, with a field-of-view of the broad beam from -20.63˚ to 20.63˚. The range resolution of the wide beam is assumed to be close to the theoretical resolution of the overall bandwidth of 1.5 cm. The main challenge for this radar system based, due to the small antenna aperture, is the cross-range or angular resolution, for which a combination of the information of the two-beam shapes, both scanning in azimuth by frequency sweeping, is utilized.

III. Radar Scenario Simulation

For verifying the performance of the proposed radar concept, a radar simulator was implemented in MATLAB, featuring arbitrary positioning of multiple antennas with individual phase,

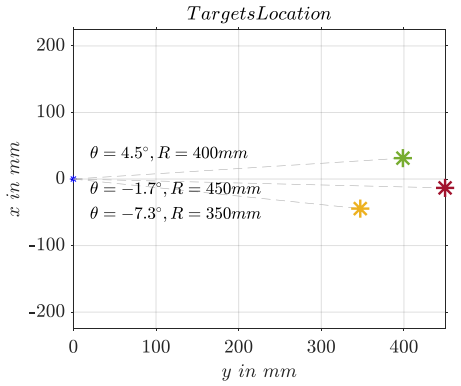

Fig. 2. A multi-target scenario for training and testing the proposed radar system algorithms.

amplitude control, and far-field radiation pattern, as well as linear-phase delay lines for the frequency-sweeping, and constant-phase phase-shifters for creating the notch, and arbitrary placement of targets modelled as point scatterers with a programmable radar cross-section. Single and multi-target scenarios were created randomly for training and testing the algorithms. Fig. 2 shows a triple targets scenario. For every scenario two frequency-dependent signals corresponding to the scanning sigma and the delta beam shapes are simulated, which are used to train and test the signal processing algorithms. For determining the angular target discrimination in multiple-target scenarios, the targets were placed within the theoretical range resolution (1.5 cm for a 10 GHz bandwidth) so that target discrimination of the algorithm by range information is be excluded.

IV. Neural Network Signal Processing Methods

Three different neural network models were implemented and benchmarked. Models A and B comprise a CNN architecture and model C is implemented as a Multilayer Perceptron (MLP). The raw data consists of a 2-dimensional data set (real and imaginary parts of the received signal), indexed by the frequency points. Each of the two beam-shapes is represented in a separate data channel. These data stream, along with the known test target positions are fed to three different machine learning models which were benchmarked for the proposed radar concept. To mitigate overfitting due to the inherent intricate structure of such problems, the input data is normalized in the range [0, 1] and a Batch Normalization layer [23] was employed among the network layers.

The internal structure of model A is different from model B, since for model A, a single 3D input stream (3D image) is created by combining the two 2D datasets of the beam shapes as two discrete channels of an image, whereas model B is fed with the two separate 2D data sets (2D images). For model C, the neural network's input stages are further simplified by combing all input data into a single, plain-value, vector. Models A and B were implemented for detecting up to two targets (2 target position outputs), whereas model C was implemented for detecting up to three targets (3 target position outputs). The two CNN models learn to select useful frequencies by weighing them over others through an iterative training process based on a Backpropagation algorithm [22]. Based on a 3-dimensional internal network structure, model A is less sensitive to noise and faulty data. Models A and B were trained for single and dual targets with up to 62000 training data sets composed of 80% training, 10% validation, and 10% test datasets. The minimum square error (MSE) to the known reference data (known target positions of the training sets) was used as the error metric for the optimization of the back-propagation algorithm. After 50 epochs of the training process, the network was finally used for predicting multi-target scenarios with target positions unknown to the machine. Model B has a higher degree of generalization than model A and can be trained simultaneously for single and multiple targets. Notwithstanding more sensitivity to signal noise and faulty data, model B results in Table 1 indicate a better generalization in determining angles for scenarios in which the model has no a-prior information on the number of targets. Model C is an MLP model [23], characterized by a much simpler structure and reduced computation complexity, using only a few different pre-determined frequency points. Three, five and, seven frequency points were arbitrarily chosen. For the created test scenarios, the model with only three frequency points

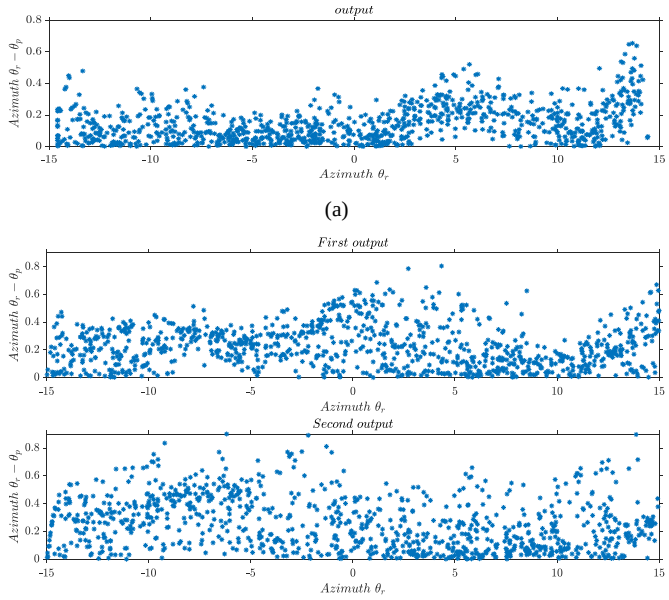

(a)

(b)

Fig. 3. Prediction error results for CNN models of type A: (a) model A-1, network trained and tested with single targets only; (b) model A-2, network trained and tested with dual targets only. Deviation of predicted angle,θ_p to the real angle, θ_r on the y-axis, and real angle θ_r on the x-axis.

(center frequency, lower and upper limit of bandwidth) exhibited the best results, but for data of a more random nature (i.e. with high noise level), models with more frequency points might perform better. Comparing to previous models the MLP model suffers from higher noise susceptibility but provides faster computation time when computation resources are limited. Model C was only trained with 16000 or 30000 data sets, since a too large number of test data sets can cause overfitting of this type of simplified model

V. Results

To evaluate the proposed neural network models, a Root Mean Square Error (RMSE) criterion is introduced, validating the deviation to the known target positions of the training data sets, as shown in equation (1). Also, a Prediction Error (PE), which is defined by equation (2), is calculated as standard error.

$$PE = \frac{1}{N}\sqrt{\sum_{i=1}^{N}(target_i - output_i)^2} \quad (1)$$

$$RMSE = \sqrt{\frac{1}{N}\sum_{i=1}^{N}(target_i - output_i)^2} \quad (2)$$

With N the size of the test-set, $target_i$ and $output_i$ are real and predicted values of a target's angle, respectively, in the i^{th}scenario.

The CNN models (A and B) are evaluated for single and dual target scenarios. However, the structure of model A works only well when either trained and tested exclusively for single targets (resulting in model A-1) or when trained and tested exclusively for dual targets (model A-2), as shown in Fig. 3 and summarized in Table I for 1000 test sets.

In contrast to that, model B's structure provides good results when trained directly for a mixed and unknown number of

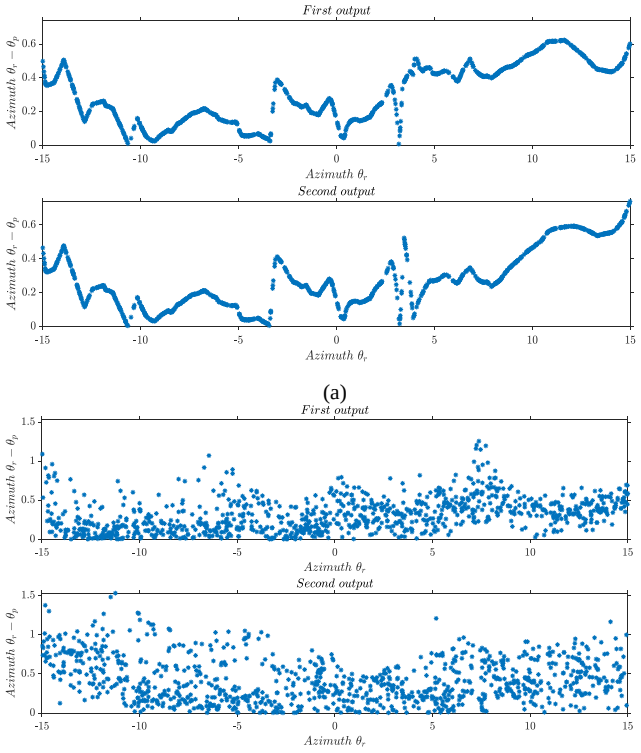

(a)

(b)

Fig. 4. Angular error results of both outputs of network B, trained for mixed single and dual target scenarios: (a) near-identical outputs when testing with single targets only; (b) prediction error for dual targets. Deviation of θ_p, θ_r on v-axis and the θ_r on the x-axis.

targets. The model can even determine the unknown number of targets, as for single targets the two outputs are expected to give near-identical values, but different values for dual targets. This is confirmed by the single-target tests shown in Fig. 4a. Fig. 4b shows that the two outputs of the model have an RMSE error of less than 0.5˚ when tested for dual targets. The results are also summarized in Table I for 1000 test sets. The overall error of model B is larger than for model variants A, which can be seen in Table I, but model B is more universally applicable since it is not limited to a specific number of targets.

Table I. PE and RMSE angular error results for networks A and B in degrees, for testing the networks both with single and dual target scenarios.

Model	Target scenario		Error first output		Error second output	
	Trained	Tested	PE	RMSE	PE	RMSE
CNN A1	single	single	0.0077	0.243	-	-
CNN A2	dual	dual	0.0087	0.2748	0.0100	0.3176
CNN B	single +dual	single	0.0107	0.3386	0.0099	0.3139
		dual	0.0121	0.3824	0.0161	0.5088

The MLP-type network C was trained simultaneously for both single and dual-targets, as model B, and also for triple-target scenarios. Table II shows the error values for model C for different dataset sizes. Although this network's error values are comparable to the CNN models of type A and B, this model, due

Table II. Angular error results (in degrees) for MLP network C, for different number of data sets and different target constellations.

Target scenarios	30000		16000	
	PE	RMSE	PE	RMSE
Single+dual	0.03	0.96	0.03	1.06
Three targets in different range*	0.07	2.48	0.08	2.63
Three targets in same range*	0.069	2.21	0.075	2.51

* within or without the range resolution of 1.5 cm.

to its structure, is more affected by the dataset size and more sensitive to noise in the data. Furthermore, another CNN model was implemented for determining the number of targets. The training and test data set comprised 96000 data for single, dual and triple target scenarios. The results of this model are shown in Fig (5) as a confusion matrix. For the 30459 test data sets, the model achieved 100% accuracy for estimating the number of targets.

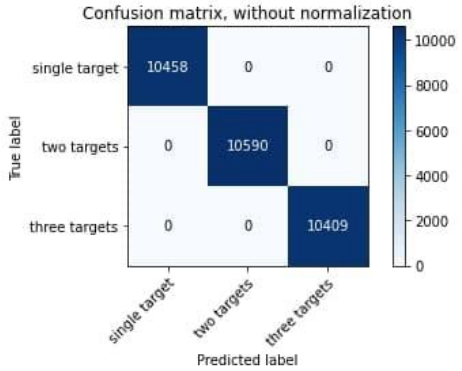

Fig. 5. The confusion matrix for testing the MLP network to predict the number of targets for 3 different scenarios.

VI. Conclusion

This paper proposed three different neural networks for single and multiple-target detection and discrimination, using the radar signal of a simulated frequency-scanning and dual beam-shape switching radar system. The lowest error in cross-range resolution can be achieved by CNN type A, but this model is applicable to a specific number of targets only. Network B can predict a mixed number of targets, still with high percision. Also, a reduced computation-complexity MLP network was investigated which benchmarked equally well to network B. When employing an estimator for the number of targets, which can be implemented with excellent accuracy as shown in this paper, the proper variant of model type A can be selected which gives the overall best results. It was shown that the proposed drastically reduced front-end size dual-antenna and dual beam-shape frequency-scanning radar system, in combination with artificial-intelligence signal processing, is able to achieve high angular accuracy and discrimination for single and multiple targets even for an unknown number of targets.

ACKNOWLEDGEMENTS

This work received funding by the European Commission through the project Car2TERA, grant agreement 842962.

References

[1] M. N. E. Korso, R. Boyer, A. Renaux, and S. Marcos, “Statistical resolution limit for source localization with clutter interference in a MIMO radar context,” *IEEE Trans. Signal Process*, vol. 60, no. 2, pp.987–992, Feb. 2012.

[2] M. D. Coco, D. Orlando, and G. Ricci, “A tracking system exploiting interaction between a detector with localization capabilities and KF,” *IEEE Trans. Signal Process*, vol. 60, no. 11, pp. 6031–6036, Nov. 2012.

[3] E. Kupershtein, M. Wax, and I. Cohen, “Single-site emitter localization via multipath fingerprinting,” *IEEE Trans. Signal Process.*, vol. 61, no.1, pp. 10–21, Jan. 2013.

[4] R. Mahajan and D. Padha, "Detection Of Concealed Weapons Using Image Processing Techniques: A Review," 2018 First International Conference on Secure Cyber Computing and Communication (ICSCCC), Jalandhar, India, 2018, pp. 375-378.

[5] J. Goodman, K. Rudd, and T. C. Clancy, “Blind multiuser localization in cognitive radio networks,” *IEEE Commun. Letter*, vol. 16, no. 7, pp 1018–1021, Jul. 2012.

[6] G. Q. Liu and J. Li, “Moving target detection via airborne HRR phasedarray radar,” *IEEE Trans. Aerosp. Electron. Syst.*, vol. 37, no. 3, pp. 914–924, Jul. 2001.

[7] J. Li and G. Q. Liu, “Moving target feature extraction for airborne highrange resolution phased-array radar,” *IEEE Trans. Signal Process*, vol. 49, no. 2, pp. 277–289, Feb. 2001.

[8] R. C. Hansen, *Microwave Scanning Antennas*, vol. 3. New York, Academic, 1966.

[9] M. Danielsen and R. Jorgensen, "Frequency scanning microstrip antennas," in IEEE Trans. on Antennas and Propagation, vol. 27, no. 2, pp. 146-150, March 1979.

[10] R. J. Mailloux, *Phased array antenna handbook*. Norwood, MA: Artech House, 2018.

[11] Z. N. Chen, D. Liu, and H. Nakano, *Handbook of antenna technologies*. Singapore: Springer Reference, 2016.

[12] A. Gomez-Torrent et al., "A Low-Profile and High-Gain Frequency Beam Steering Subterahertz Antenna Enabled by Silicon Micromachining," in IEEE Trans. on Antennas and Propagation, vol. 68, no. 2, pp. 672-682, Feb. 2020.

[13] M. Ettorre, A. Neto, G. Gerini and S. Maci, "Leaky-wave slot array antenna fed by a dual reflector system", *IEEE Trans. Antennas Propag.*, vol. 56, no. 10, pp. 3143-3149, Oct. 2008.

[14] T. Djerafi and K. Wu, "A low-cost wideband 77-GHz planar Butler matrix in SIW technology", *IEEE Trans. Antennas Propag.*, vol. 60, no. 10, pp. 4949-4954, Oct. 2012.

[15] M. Ettorre, R. Sauleau, L. L. Coq and F. Bodereau, "Single-folded leaky-wave antennas for automotive radars at 77 GHz", *IEEE Antennas Wireless Propag. Letter*, vol. 9, pp. 859-862, 2010.

[16] V. S. Chernyak, *Fundamentals of multisite radar systems: multistatic radars and multiradar systems*. Amsterdam, the Netherlands: Gordon and Breach Science Publishers, 1998.

[17] S. M. Sherman and D. K. Barton, *Monopulse principles and techniques*. Boston: Artech House, 2011.

[18] Y. Zhang, A. S. Venkatachalam, D. Huston, and T. Xia, "Advanced signal processing method for ground penetrating radar feature detection and enhancement," in *Nondestructive Characterization for Composite Materials 2014*, vol. 9063,, p. 906318.

[19] L. Li *et al.*, "DeepNIS: Deep neural network for nonlinear electromagnetic inverse scattering," vol. 67, no. 3, pp. 1819-1825, 2018.

[20] V. J. a. p. a. Puzyrev, "Deep learning electromagnetic inversion with convolutional neural networks. Submitted," 2018.

[21] S. Hazra and A. J. I. s. l. Santra, "Robust gesture recognition using millimetric-wave radar system," vol. 2, no. 4, pp. 1-4, 2018.

[22] D. E. Rumelhart, G. E. Hinton, and R. J. J. n. Williams, "Learning representations by back-propagating errors," vol. 323, no. 6088, pp. 533-536, 1986.

[23] L. V. Fausett, Fundamentals of neural networks: architectures, algorithms and applications. Pearson Education India, 2006.